International Journal of Pharmaceutics 481 (2015) 64–70

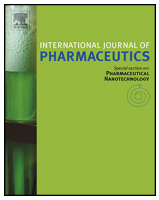

Three-dimensional analyses of a perforated cylindrical drug delivery device

Laurent Simon [a,*], Juan Ospina [b]

[a] Otto H. York Department of Chemical, Biological and Pharmaceutical Engineering, New Jersey Institute of Technology, Newark, NJ 0702, USA
[b] Logic and Computation Group, Physics Engineering Program, School of Sciences and Humanities, EAFIT University, Medellin, Colombia

ARTICLE INFO

Article history:
Received 4 November 2014
Received in revised form 27 December 2014
Accepted 24 January 2015
Available online 28 January 2015

Keywords:
Three-dimensional model
Effective time constant
Cylindrical device
Residue theorem
Controlled release

ABSTRACT

A closed-formed solution of a perforated drug-delivery model was developed. Laplace transforms were applied to the governing equation, which included diffusion through the tubular device and mass transfer across a rectangular cut. A first-order estimate for the fraction of drug released, in terms of the Laplace variable, was derived after employing suitable boundary and initial conditions. The effective time constant for the process was calculated. The residue theorem and the Zakian method were proposed as two reliable approaches to recover the solution in the time domain. Simulations show that the drug was released faster at higher Sherwood numbers. Ninety-eight percent (98%) of the loading dose was delivered after a period corresponding to four time constants. This analytical platform can aid in the design of implants for long-term delivery applications.

1. Introduction

1.1. Design of controlled-release systems

Controlled-release (CR) drug-delivery systems are designed to administer an exact dosage of an active pharmaceutical ingredient (API) to a target site during a treatment period. Contrary to a sustained release, which simply prolongs the drug action, CR technologies involve the regulation of the time course of the therapeutic agent while it is being delivered to a particular location. The kinetics, e.g., Higuchi, zero-order or first-order, are pertinent to the design of CR devices (Prasanna and Sankari, 2012; Verma and Iyer, 2000). In the manufacturing of these pharmaceutical products, the excipients, used to achieve the desired kinetics, are mainly composed of polymers with finely-tuned physicochemical properties. Patel and coworkers described a time- and pH-dependent delivery system to supply mesalamine to the colon (Patel et al., 2009). The goal was to prevent early release of the API in the small intestine before it reaches its destination. Using statistical methods, the composition of the inner coating was optimized to reach specific values of the lag time and t_{50}, i.e., the time required to unload 50% of the drug. Zhao and colleagues note that the kinetics of drug-eluting stents can be regulated by manipulating parameters, such as the diffusion coefficient and the coating thickness (Zhao et al., 2012). A cylindrical diffusion mathematical model was applied to represent permeation of the molecules through the outer polymer shell. Their work demonstrates the importance of rigorous modeling in the development of CR devices.

1.2. One-dimensional representation of controlled-release systems

Mathematical modeling continues to play an important role in the design of controlled delivery systems. The work of Higuchi (Higuchi, 1961) is often cited as the starting point for using equations to describe drug transport from polymer matrices. A one-dimensional (1-D) analysis was conducted and a constant diffusivity was assumed in the original work. According to the model, the percentage of drug permeated is proportional to the square root of time. Fickian and non-Fickian diffusions from swelling and non-swelling polymers were later considered (Korsmeyer et al., 1986; Ritger and Peppas, 1987). These expressions are largely applied in research on hydrogels to clarify the mechanisms controlling the delivery rate (Lin and Metters, 2006). The 1-D approach is also useful in depicting drug permeation through the skin (Fernandes et al., 2005; Guy and Hadgraft, 1980; Kalia and Guy, 2001). This procedure yields relatively simple equations that are proposed to calculate meaningful constants, such as the lag time and diffusion coefficient. Development of algebraic expressions to estimate an effective time constant (Simon, 2009) or the time required for drugs in suspension to dissolve (Bunge, 1998) is also allowed in this framework. Solutions for these problems are discussed in Crank (1975) and Kim (2000).

* Corresponding author. Tel.: +1 973 596 5263; fax: +1 973 596 8436.
E-mail address: laurent.simon@njit.edu (L. Simon).

http://dx.doi.org/10.1016/j.ijpharm.2015.01.047
0378-5173/

1.3. Two-dimensional representation of controlled-release systems

Two-dimensional models are required to represent, adequately, the release profile from some matrix devices. Tojo and Miyanami developed a 2-D structure to assess the effects of design criteria, such as the release hole radius, on the fraction of drug accumulated (Tojo and Miyanami, 1983). This model could predict the delivery of benzoic acid from a cylindrical agar gel. A closed-form solution was derived using a Laplace transform-based technique (Simon and Ospina, 2012). This analytical approach provided further insight into the influences of geometries and polymer properties on the performance of the device. Simulations, conducted by Davia et al., proved that the release kinetics of nucleic acid-based drugs from endoluminal gel-paved stents could be manipulated by changing the diffusivity of the medicament-carrier complex (Davia et al., 2009). Desired changes are made in selecting carriers with suitable dimensions. Diffusion took place in the radial and axial coordinates. Siepmann et al. adopted a similar framework to study water transport and drug release from hydroxypropyl methylcellulose (HPMC) tablets (Siepmann et al., 1999). The numerical solution of the governing partial differential equations helped to link the profile to the shape and dimensions of the tablets. A finite-element analysis was performed to study slowly-dissolving drugs in cylindrical matrices (Frenning et al., 2005). The dissolution rate may have an impact on drug transport.

1.4. Three-dimensional representation of controlled-release systems

Frenning and coworkers noticed that published research mainly focuses on planar geometries or systems that are satisfactorily described by one-dimensional equations (Frenning et al., 2005). When edge effects are important, a three-dimensional diffusion equation is warranted (Ainaoui et al., 2001; Vergnaud and Rosca, 2005). The fraction of the diffusing agent collected in a receiver compartment is calculated by taking the product of three-series solutions corresponding to transport through flat membranes. Two-series solutions could be employed to two dimensions. This approach can be applied to drug loaded in a cube. The method does not extend to implantable cylindrical matrices with release holes located on the surface of the design (Ertan et al., 1997; Hsu et al., 1992). Even with the assumption of angular symmetry, the concentration distribution is not easily obtained through the above-mentioned technique (Simon and Ospina, 2012). Analytical tools are lacking in the literature to study drug mechanisms in 3-D coordinates. A 3-D solution for the amount of medication released from a cylindrical device is considered throughout this work. The perforation is along the cylinder while the rest of the tube is coated in such a way that the drug is released only through the hole. The proposed design is motivated by a delivery system developed in (Rastogi et al., 2012, 2010). These researchers studied the controlled release of fluorescein, crystal violet and ethinyl estradiol from polyimide microtubes. The main difference between the system studied in Rastogi et al. (2012, 2010) and the one considered in this work is that the microhole on the surface of the tube is now shaped like a rectangle.

2. Materials and methods

2.1. Mathematical modeling

The system studied in this contribution is a cylindrical, monolithic structure which contains an active agent *A*. The CR device is covered by an impermeable coating substance and the medication is released through a small cylindrical rectangle located on the lateral surface (Fig. 1). Experiments were performed using polyimide tubings (Rastogi et al., 2012).

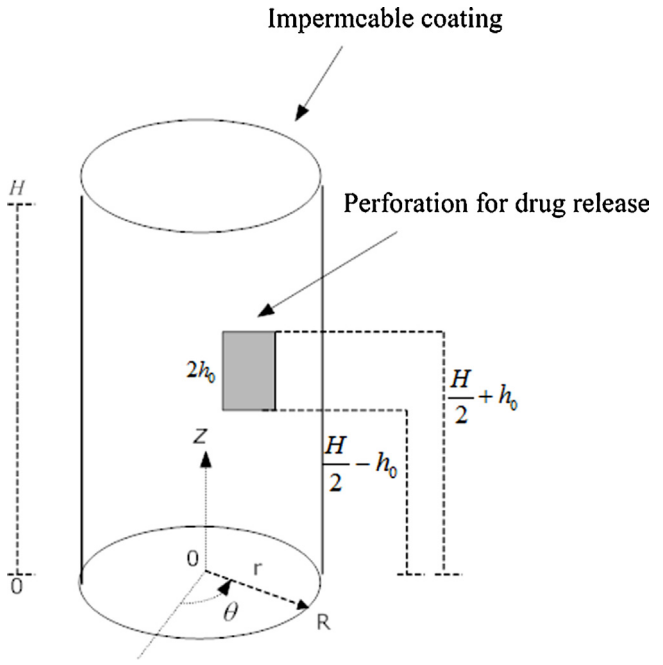

Fig. 1. Dimensions of the cylindrical drug-delivery system.

A balance on component *A* gives

$$\frac{\partial C_A(t,r,\theta,z)}{\partial t} = \eta_A\left[\frac{\partial^2 C_A(t,r,\theta,z)}{\partial r^2}+\frac{1}{r}\frac{\partial C_A(t,r,\theta,z)}{\partial r}+\frac{1}{r^2}\frac{\partial^2 C_A(t,r,\theta,z)}{\partial \theta^2}+\frac{\partial^2 C_A(t,r,\theta,z)}{\partial z^2}\right] \quad (1)$$

where $C_A(t,r,\theta,z)$ denotes the concentration of *A* located at the point (r,θ,z) and η_A is the drug diffusion coefficient in the matrix. Eq. (1) represents Fick's second law of diffusion in cylindrical coordinates. It explains random molecular motion from a region of high concentration to an area of low concentration. Diffusion takes place in all three directions.

The initial condition is

$$C_A(0,r,\theta,z) = C_{AS} \quad (2)$$

where C_{AS} is the saturated concentration of *A* in the matrix. The boundary conditions are

$$\frac{\partial C_A(t,r,\theta,z)}{\partial z}\Big|_{z=0} = 0 \quad (3)$$

$$\frac{\partial C_A(t,r,\theta,z)}{\partial z}\Big|_{z=H} = 0 \quad (4)$$

$$\frac{\partial C_A(t,r,\theta,z)}{\partial r}\Big|_{r=R} = \begin{cases} -\frac{k_m}{\eta_A}C_A(t,R,\theta,z) & \frac{H}{2}-h_0 \le z \le \frac{H}{2}+h_0,\ 0<\theta<\Theta_0 \\ 0 & \text{otherwise} \end{cases} \quad (5)$$

According to the conditions defined in Eqs. (3)–(5) , the drug is released only through the small cylindrical rectangle, of radius *R* with angular aperture Θ_0, located between the planes $z=(H/2)-h_0$ and $z=(H/2)+h_0$. The parameter k_m indicates a boundary-layer mass transfer coefficient. A high k_m implies a low-mass transfer

resistance which may be the result of factors, such as a strong mixing. A low k_m value would hamper the delivery of the drug into the surrounding environment.

Eqs. (1)–(5) are written in the following dimensionless form:

$$\frac{\partial C(\tau,\rho,\theta,\zeta)}{\partial \tau} = \eta_A\left[\frac{\partial^2 C(\tau,\rho,\theta,\zeta)}{\partial \rho^2}+\frac{1}{\rho}\frac{\partial C(\tau,\rho,\theta,\zeta)}{\partial \rho}+\frac{1}{\rho^2}\frac{\partial^2 C(\tau,\rho,\theta,\zeta)}{\partial \theta^2}+\frac{\partial^2 C(\tau,\rho,\theta,\zeta)}{\partial \zeta^2}\right] \tag{6}$$

$$C(0,\rho,\theta,\zeta)=1 \tag{7}$$

$$\frac{\partial C(\tau,\rho,\theta,\zeta)}{\partial \zeta}\Big|_{\zeta=0}=0 \tag{8}$$

$$\frac{\partial C(\tau,\rho,\theta,\zeta)}{\partial \zeta}\Big|_{\zeta=\frac{H}{R}}=0 \tag{9}$$

$$\frac{\partial C(\tau,\rho,\theta,\zeta)}{\partial \zeta}\Big|_{\zeta=1}=\begin{cases}-ShC(\tau,1,\theta,\zeta) & \frac{H}{2R}-\frac{h_0}{R}\le\zeta\le\frac{H}{2R}+\frac{h_0}{R},\ 0<\theta<\Theta_0\\ 0 & \text{otherwise}\end{cases} \tag{10}$$

The dimensionless variables and constants which appear in Eqs. (6)–(10) are defined as follows:

$$\rho=\frac{r}{R},\ \zeta=\frac{z}{R},\ \tau=\frac{t\eta_A}{R^2},\ C(\tau,\rho,\theta,\zeta)=\frac{C_A(t,r,\theta,z)}{C_{AS}},\ Sh=\frac{Rk_m}{\eta_A} \tag{11}$$

The Sherwood number Sh is a dimensionless number that stands for the ratio of convective to diffusive mass transfer.

2.2. Derivation of the concentration profile in the frequency domain

The first steps in developing an analytical solution of the dimensionless problem, defined by Eqs. (6)–(10), is to use Laplace transform techniques. The computations are done in Maple (Waterloo Software Inc.). Taking the Laplace transform of Eq. (6) and applying the initial condition (7) results in

$$s\overline{C}(s,\rho,\theta,\zeta)-1=\eta_A\left[\frac{\partial^2\overline{C}(s,\rho,\theta,\zeta)}{\partial\rho^2}+\frac{1}{\rho}\partial\frac{\overline{C}(s,\rho,\theta,\zeta)}{\partial\rho}+\frac{1}{\rho^2}\frac{\partial^2\overline{C}(s,\rho,\theta,\zeta)}{\partial\theta^2}+\frac{\partial^2\overline{C}(s,\rho,\theta,\zeta)}{\partial\zeta^2}\right] \tag{12}$$

The general solution of Eq. (12) is

$$\overline{C}(s,\rho,\theta,\zeta)=F_1(s,\rho)F_2(s,\zeta)F_3(s,\theta)+\frac{1}{s} \tag{13}$$

where

$$F_1(s,\rho)=d_1J_{\sqrt{-c_2}}(\rho\sqrt{c_3-s})+d_2Y_{\sqrt{-c_2}}(\rho\sqrt{c_3-s})$$
$$F_2(s,\zeta)=\frac{d_3e^{2\zeta\sqrt{c_3}}+d_4}{e^{\zeta\sqrt{c_3}}} \tag{14}$$
$$F_3(s,\theta)=\frac{d_5e^{2\theta\sqrt{c_2}}+d_6}{e^{\theta\sqrt{c_2}}}$$

In Eq. (14), J and Y represent Bessel functions of the first and second kind, respectively; d_1, d_2,d_3, d_4, d_5, d_6, c_2 and c_3 are constants to be calculated using the boundary conditions. Because $Y_{\sqrt{-c_2}}(x)$ is singular around $x=0$, the constant d_2 should be zero for a finite solution at $\rho=0$. Without any loss of generality, d_1 is set equal to 1 which yields

$$\overline{C}(s,\rho,\theta,\zeta)=J_{\sqrt{-c_2}}(\rho\sqrt{c_3-s})\left(\frac{d_3e^{2\zeta\sqrt{c_3}}+d_4}{e^{\zeta\sqrt{c_3}}}\right)\left(\frac{d_5e^{2\theta\sqrt{c_2}}+d_6}{e^{\theta\sqrt{c_2}}}\right)+\frac{1}{s} \tag{15}$$

After applying Eq. (8), Eq. (15) gives

$$\left(d_5e^{2\theta\sqrt{c_2}}+d_6\right)\sqrt{c_3}J_{\sqrt{-c_2}}(\rho\sqrt{c_3-s})(d_3-d_4)e^{-\theta\sqrt{c_2}}=0 \tag{16}$$

implying that $d_3=d_4$. As a result, we have

$$\overline{C}(s,\rho,\theta,\zeta)=J_{\sqrt{-c_2}}(\rho\sqrt{c_3-s})\left(\frac{d_3e^{2\zeta\sqrt{c_3}}+d_3}{e^{\zeta\sqrt{c_3}}}\right)\left(\frac{d_5e^{2\theta\sqrt{c_2}}+d_6}{e^{\theta\sqrt{c_2}}}\right)+\frac{1}{s} \tag{17}$$

Application of Eq. (9) leads to

$$2d_3\sqrt{c_3}\left(d_5e^{2\theta\sqrt{c_2}}+d_6\right)J_{\sqrt{-c_2}}(\rho\sqrt{c_3-s})e^{-\theta\sqrt{c_2}}\sinh\left(\frac{H\sqrt{c_3}}{R}\right)=0 \tag{18}$$

The equality $\sinh(H\sqrt{c_3}/R)=0$ admits an infinite number of imaginary roots $H\sqrt{c_3}/R=n\pi i$ or $c_3=-n^2\pi^2R^2/H^2$. Eq. (17) becomes

$$\overline{C}(s,\rho,\theta,\zeta)=2d_3\left(d_5e^{2\theta\sqrt{c_2}}+d_6\right)e^{-\theta\sqrt{c_2}}\cos\left(\frac{n\pi R\zeta}{H}\right)\times J_{i\sqrt{c_2}}\left(\frac{i\rho\sqrt{n^2\pi^2R^2+sH^2}}{H}\right)+\frac{1}{s} \tag{19}$$

where n is an integer ranging from 0 to ∞. Given that the cylindrical variable θ belongs to the range $[0,2\pi]$, Eq. (19) must be a periodic function of θ with a period of 2π. As a result, the condition $c_2=-m^2$ is fitting where m is also an integer from 0 to ∞. Then, Eq. (19) takes the form:

$$\overline{C}(s,\rho,\theta,\zeta)=2\cos\left(\frac{n\pi R\zeta}{H}\right)J_m\left(\frac{i\rho\sqrt{n^2\pi^2R^2+sH^2}}{H}\right)\times\left(d_5e^{-m\theta i}+d_6e^{m\theta i}\right)+\frac{1}{s} \tag{20}$$

after setting $d_3=1$. The use of the superposition principle results in

$$\overline{C}(s,\rho,\theta,\zeta)=\frac{1}{s}+2\sum_{n=0}^{\infty}\left[\sum_{m=0}^{\infty}\cos\left(\frac{n\pi R\zeta}{H}\right)J_m\left(\frac{i\rho\sqrt{n^2\pi^2R^2+sH^2}}{H}\right)\times\left(A_{n,m}\cos(m\theta)+B_{n,m}\sin(m\theta)\right)\right] \tag{21}$$

which is rewritten as

$$\begin{aligned}\overline{C}(s,\rho,\theta,\zeta)=&\frac{1}{s}+2I_0(\rho\sqrt{s})A_{0,0}\\&+2\sum_{m=1}^{\infty}J_m(i\rho\sqrt{s})\left(A_{0,m}\cos(m\theta)+B_{0,m}\sin(m\theta)\right)\\&+2\sum_{n=1}^{\infty}\cos\left(\frac{n\pi R\zeta}{H}\right)I_0\left(\frac{\rho\sqrt{n^2\pi^2R^2+sH^2}}{H}\right)A_{n,0}\\&+2\sum_{n=1}^{\infty}\left[\sum_{m=1}^{\infty}\cos\left(\frac{n\pi R\zeta}{H}\right)J_m\left(\frac{i\rho\sqrt{n^2\pi^2R^2+sH^2}}{H}\right)\times\left(A_{n,m}\cos(m\theta)+B_{n,m}\sin(m\theta)\right)\right]\end{aligned} \tag{22}$$

where I is the modified Bessel function of the first kind. The following equality is obtained after substituting Eq. (10) into Eq. (22):

$$
\begin{aligned}
&2I_1(\sqrt{s})\sqrt{s}A_{0,0}+2i\left[-J_2\left(i\sqrt{s}\right)-\frac{iJ_1(i\sqrt{s})}{\sqrt{s}}\right]\sqrt{s}(A_{0,1}\cos(\theta)+B_{0,1}\sin(\theta))\\
&+\frac{2\cos\left(\frac{\pi R\zeta}{H}\right)I_1\left(\frac{\sqrt{\pi^2R^2+sH^2}}{H}\right)\sqrt{\pi^2R^2+sH^2}A_{1,0}}{H}\\
&+\left\{\begin{array}{l}\frac{1}{H}2i\cos\left(\frac{\pi R\zeta}{H}\right)\left[-J_2\left(\frac{i\sqrt{\pi^2R^2+sH^2}}{H}\right)-\frac{iHJ_1\left(\frac{i\sqrt{\pi^2R^2+sH^2}}{H}\right)}{\sqrt{\pi^2R^2+sH^2}}\right]\\ \times\sqrt{\pi^2R^2+sH^2}(A_{1,1}\cos(\theta)+B_{1,1}\sin(\theta))\end{array}\right\}\\
&=-Sh\begin{cases}\begin{array}{l}\frac{1}{s}+2I_0\left(\sqrt{s}\right)A_{0,0}\\ +2J_1\left(i\sqrt{s}\right)(A_{0,1}\cos(\theta)+B_{0,1}\sin(\theta))\\ +2\cos\left(\frac{\pi R\zeta}{H}\right)I_0\left(\frac{\sqrt{\pi^2R^2+sH^2}}{H}\right)A_{1,0}\\ +\left[\begin{array}{l}2\cos\left(\frac{\pi R\zeta}{H}\right)J_1\left(\frac{i\sqrt{\pi^2R^2+sH^2}}{H}\right)\\ \times(A_{1,1}\cos(\theta)+B_{1,1}\sin(\theta))\end{array}\right]\end{array} & \frac{H}{2R}-\frac{h_0}{R}\le\zeta\le\frac{H}{2R}+\frac{h_0}{R},\ 0<\theta<\Theta_0\\ 0 & \text{otherwise}\end{cases}
\end{aligned}
\tag{23}
$$

Eq. (23) is a large expression that is difficult to manipulate. We search for a first-order approximation (i.e., $n=m=1$) of the form:

$$
\begin{aligned}
&2I_1(\sqrt{s})\sqrt{s}A_{0,0}+2i\left[-J_2\left(i\sqrt{s}\right)-\frac{iJ_1(i\sqrt{s})}{\sqrt{s}}\right]\sqrt{s}(A_{0,1}\cos(\theta)+B_{0,1}\sin(\theta))\\
&+\frac{2\cos\left(\frac{\pi R\zeta}{H}\right)I_1\left(\frac{\sqrt{\pi^2R^2+sH^2}}{H}\right)\sqrt{\pi^2R^2+sH^2}A_{1,0}}{H}\\
&+\left\{\begin{array}{l}\frac{1}{H}2i\cos\left(\frac{\pi R\zeta}{H}\right)\left[-J_2\left(\frac{i\sqrt{\pi^2R^2+sH^2}}{H}\right)-\frac{iHJ_1\left(\frac{i\sqrt{\pi^2R^2+sH^2}}{H}\right)}{\sqrt{\pi^2R^2+sH^2}}\right]\\ \times\sqrt{\pi^2R^2+sH^2}(A_{1,1}\cos(\theta)+B_{1,1}\sin(\theta))\end{array}\right\}=\\
&\left[-Sh\begin{cases}\begin{array}{l}\frac{1}{s}+2I_0\left(\sqrt{s}\right)A_{0,0}\\ +2J_1\left(i\sqrt{s}\right)(A_{0,1}\cos(\theta)+B_{0,1}\sin(\theta))\\ +2\cos\left(\frac{\pi R\zeta}{H}\right)I_0\left(\frac{\sqrt{\pi^2R^2+sH^2}}{H}\right)A_{1,0}\\ +\left[\begin{array}{l}2\cos\left(\frac{\pi R\zeta}{H}\right)J_1\left(\frac{i\sqrt{\pi^2R^2+sH^2}}{H}\right)\\ \times(A_{1,1}\cos(\theta)+B_{1,1}\sin(\theta))\end{array}\right]\end{array} & \frac{H}{2R}-\frac{h_0}{R}\le\zeta\le\frac{H}{2R}+\frac{h_0}{R},\ 0<\theta<\Theta_0\\ 0 & \text{otherwise}\end{cases}\right]
\end{aligned}
\tag{24}
$$

Several integrations are performed to find the coefficients (see Appendix A). The system formed by Eqs. (A.1)–(A.6) is solved for $A_{0,0}$, $A_{0,1}$, $B_{0,1}$, $A_{1,0}$, $A_{1,1}$ and $B_{1,1}$ (results not shown). Consequently, the first-order approximation to Eq. (22) is given by

$$
\begin{aligned}
\overline{C}(s,\rho,\theta,\zeta)=&\frac{1}{s}+2I_0(\rho\sqrt{s})A_{0,0}+2J_1(i\rho\sqrt{s})(A_{0,1}\cos(\theta)+B_{0,1}\sin(\theta))\\
&+2\cos\left(\frac{\pi R\zeta}{H}\right)I_0\left(\frac{\rho\sqrt{\pi^2R^2+sH^2}}{H}\right)A_{1,0}\\
&+2\cos\left(\frac{\pi R\zeta}{H}\right)J_1\left(\frac{i\rho\sqrt{\pi^2R^2+sH^2}}{H}\right)(A_{1,1}\cos(\theta)+B_{1,1}\sin(\theta))
\end{aligned}
\tag{25}
$$

2.3. Derivation of the cumulative amount of drug released

The cumulative amount of API collected in the receiver compartment at time t, denoted $M(t)$, is the difference between the initial drug loading and the amount remaining at time t:

$$
M(t)=C_{AS}\pi R^2H-\int_0^{2\pi}\int_0^{H}\int_0^{R}C_A(t,r,\theta,z)\mathrm{d}r\mathrm{d}z\mathrm{d}\theta \tag{26}
$$

Eq. (26) is recast in terms of dimensionless variables as

$$
M(\tau)=C_{AS}\pi R^2H-C_{AS}R^3\int_0^{2\pi}\int_0^{\frac{H}{R}}\int_0^{1}C(\tau,\rho,\theta,\zeta)\rho\mathrm{d}\rho\mathrm{d}\zeta\mathrm{d}\theta \tag{27}
$$

The normalized form of Eq. (27) is

$$
\frac{M(\tau)}{M(\infty)}=1-\left(\frac{R}{\pi H}\int_0^{2\pi}\int_0^{\frac{H}{R}}\int_0^{1}C(\tau,\rho,\theta,\zeta)\rho\mathrm{d}\rho\mathrm{d}\zeta\mathrm{d}\theta\right) \tag{28}
$$

where $M(\infty)=C_{AS}\pi R^2H$. The Laplace transform of Eq. (28) is

$$
\frac{\overline{M}(s)}{M(\infty)}=\frac{1}{s}-\left(\frac{R}{\pi H}\int_0^{2\pi}\int_0^{\frac{H}{R}}\int_0^{1}\overline{C}(s,\rho,\theta,\zeta)\rho\mathrm{d}\rho\mathrm{d}\zeta\mathrm{d}\theta\right) \tag{29}
$$

or

$$
\frac{\overline{M}(s)}{M(\infty)}=\frac{1}{s}-\frac{R}{\pi H}\left(\int_0^{2\pi}\int_0^{\frac{H}{R}}\int_0^{1}\overline{C}(s,\rho,\theta,\zeta)\rho\mathrm{d}\rho\mathrm{d}\zeta\mathrm{d}\theta\right) \tag{30}
$$

with $\overline{C}(s,\rho,\theta,\zeta)$ defined by Eq. (25). After computing the integrals in Eq. (30) and simplifying, the following equation is obtained:

$$
\frac{\overline{M}(s)}{M(\infty)}=-\frac{4A_{0,0}I_1(\sqrt{s})}{\sqrt{s}} \tag{31}
$$

Numerous techniques are available to invert Eq. (31) in the time domain. Two of these procedures are outlined here. The Residue theorem (Loney, 2007) produces

$$
\frac{M(\tau)}{M(\infty)}=1-\sum_{n=1}^{\infty}\left(\frac{4P(\alpha_n)I_1(\sqrt{\alpha_n})e^{\alpha_n\tau}}{\frac{d}{ds}(\sqrt{s}Q(s))|_{s=\alpha_n}}\right) \tag{32}
$$

where $P(s)$ and $Q(s)$ are such that $A_{0,0}=P(s)/Q(s)$ and α_n are the roots of $Q(s)=0$.

Another option is the implementation of the Zakian method (Rice and Do, 1995):

$$
\frac{M(\tau)}{M(\infty)}=\frac{2}{\tau}\sum_{i=1}^{5}Re\left(K_i\frac{M(a_i/\tau)}{M(\infty)}\right) \tag{33}
$$

where K_i and a_n are complex numbers defined in the Zakian algorithm. The latter procedure is preferred in this work because it is easier to implement, less computationally expensive than the Residue theorem and does not require the calculation of the roots.

2.4. Derivation of the effective time constant

It is important to drug manufacturers to design CR devices so that the API is delivered at a desired speed. Therefore, the notion of a time constant is necessary to the effectiveness of the product. The method suggested by Collins is followed (Collins, 1980). This parameter is derived from the concentration profile $C_A(t,r,\theta,z)$. The effective relaxation time is defined by

$$
\tau_{\mathrm{eff}}=\int_0^{\infty}\tau\Omega(\tau)\mathrm{d}\tau \tag{34}
$$

where the probability density function $\Omega(\tau)$ is

$$
\Omega(\tau)=\frac{(g_e-g(\tau))}{\int_0^{\infty}(g_e-g(\tau))\mathrm{d}\tau} \tag{35}
$$

Eq. (34) is written in terms of Laplace variables as

$$\tau_{\text{eff}} = \lim_{s\to 0}\left(\frac{\Psi_{\text{ss}}}{s^2} + \frac{d\overline{\Psi}(s)}{ds}\right)\left[\lim_{s\to 0}\left(\frac{\Psi_{\text{ss}}}{s} - \overline{\Psi}(s)\right)\right]^{-1} \tag{36}$$

where Ψ_{ss} is the steady-state value and $\overline{\Psi}$ is the Laplace transform of Ψ. Eq. (36) is applied to Eq. (31) (i.e., $\Psi = M(\tau)/M(\infty)$ to yield τ_{eff} in terms of the device properties. This metric was adopted in previous contributions to evaluate the dynamic behavior of CR systems (Simon, 2009).

3. Results and discussions

3.1. Model validation

In-vitro release data were obtained from Rastogi et al. (2012) to validate the model. An average amount of 34.6 ± 1.6 mg of a mixture of sodium fluorescein and stearic acid was loaded in the tubes. Fig. 2 corresponds to a 50:50 fluorescein and stearic acid ratio. The length and inside diameter of the polyimide tubing was 20 mm and 0.18 mm, respectively. A circular hole of 1.15 mm in diameter was made. These dimensions were first tailored to match those of an equivalent cylindrical cut. Note that r is the radius of the hole, R is the radius of the cylinder and θ is the angular position. It can be shown that the cylindrical hole has the following dimensions: $\theta = (r/R)\sqrt{\pi};\ 2h_0 = r\sqrt{\pi}$. The experimental percentage of sodium fluorescein released was plotted by dividing the cumulative amount given in Rastogi et al. (2012) by a load of 17.3 mg (i.e., 50:50 fluorescein and stearic acid ratio). These data were fitted to the theoretical model (Eq. 33) using a regression technique in Mathematica (Wolfram Research, Inc.). The best diffusion and mass transfer coefficients were 1.98×10^{-6} cm^2/s and 3.23×10^{-4} cm/s. The theoretical results agree with the theoretical predictions (Fig. 2).

3.2. Simulation results

The Sherwood number represents a resistance to mass transfer into the environment across a boundary layer that is adjacent to the device. Fig. 3 summarizes the effect of the Sherwood number on $M(\tau)/M(\infty)$ and τ_{eff}. A high Sh signifies a well-mixed condition and a low Sh is the result of poor mixing. The angle Θ_0 was set at $\pi/8$ for the simulation. This plot was drawn using the geometric

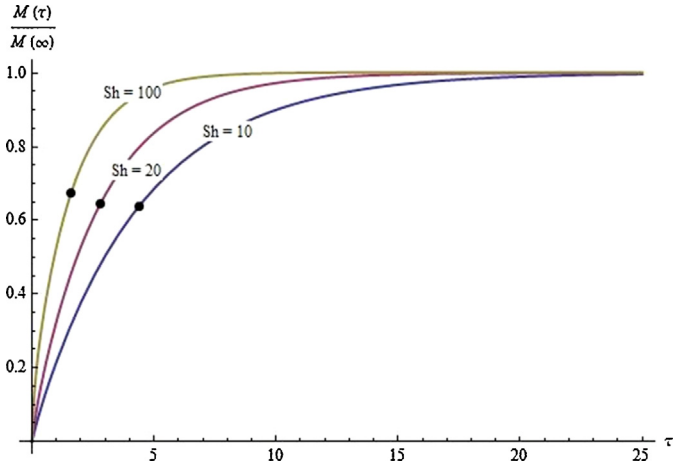

Fig. 3. The fraction of drug released $M(\tau)/M(\infty)$ and the effective time constant τ_{eff} (●) at three Sherwood numbers. The following parameters were defined for the simulation $\Theta_0 = \pi/8$, $\gamma = 2$ and $\chi = 0.25$.

ratios $\gamma = H/R$ and $\chi = h_0/H$ and the following values $\gamma = 2$ and $\chi = 0.25$. The cumulative amount of drug released, over time, increases with Sh. As the mass transfer is improved (i.e., vigorous mixing), more API is discharged into the surrounding fluid. The rate at which the drug leaves the hole increases (i.e., lower τ_{eff}) with a rise in Sh. When Θ_0 changes from $\pi/8$ to $\pi/2$ (Fig. 4) or χ varies from 0.10 to 0.25 (Fig. 5), the API is discharged more rapidly because of the larger release area. Although these observations could be predicted qualitatively, the numerical solution makes it feasible to examine the effects of design modifications on the system performance. Implants, that meet specific objectives, can be designed through simulations before performing the experiments. For example, a time constant of 4.37 is achieved by selecting $\chi = 0.25$, $\gamma = 2$ and $\Theta_0 = \pi/8$ and $Sh = 10$ (Fig. 3).

The time constant is also a measure of how long it takes to release the drug from the tube. A first-order process (output γ) reaches ninety-eight percent of its steady state at $4\tau_{\text{eff}}$:

$$\tau_{\text{eff}}\frac{dy}{dt} + y = K_p u(t) \tag{37}$$

where u is an input variable; τ_{eff} and K_p are the time constant and steady-state gain, respectively. Although transport, in this work, is

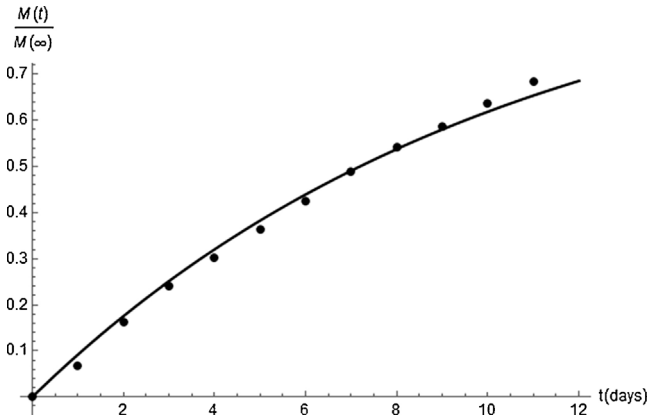

Fig. 2. In-vitro release of sodium fluorescein from a 50:50 mixture of sodium fluorescein and stearic acid (Rastogi et al., 2012). Predicted (—) and experimental (●) cumulative percentages of the drug model are shown.

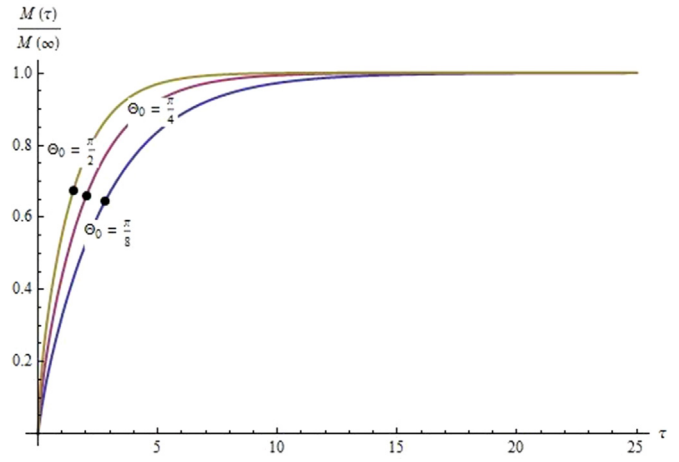

Fig. 4. The fraction of drug released $M(\tau)/M(\infty)$ and the effective time constant τ_{eff} (●) at three angles. The following parameters were defined for the simulation $Sh = 20$, $\gamma = 2$ and $\chi = 0.25$.

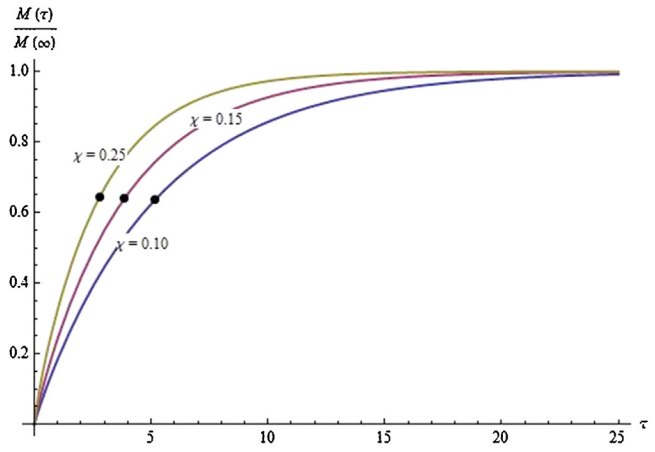

Fig. 5. The fraction of drug released $M(\tau)/M(\infty)$ and the effective time constant τ_{eff} (●) at three $\chi = h_0/H$ values. The following parameters were defined for the simulation $Sh = 20$, $\Theta_0 = \pi/8$ and $\gamma = 2$.

governed by convection and diffusion and involves several time constants (i.e., $1/\alpha_n$ in Eq. (32)), the $4\tau_{eff}$ estimation of the onset of steady state is appropriate as was shown in Simon (2009). Calculation of τ_{eff} and $M(4\tau_{eff})/M(\infty)$ gives 5.16 and 0.98, respectively, when $\chi = 0.10$, $\gamma = 2$, $\Theta_0 = \pi/8$ and $Sh = 20$ (Fig. 5). The constants, $\tau_{eff} = 1.61$ and $M(4\tau_{eff})/M(\infty) = 0.98$, are computed for the following specifications: $\chi = 0.25$, $\gamma = 2$, $\Theta_0 = \pi/8$ and $Sh = 100$ (Fig. 3). These findings agree with those published in Simon (2009).

This study raises the possibility of developing implants for long-term drug delivery. Simulated release profiles will give product manufacturers a sense of the range of specifications (e.g., size of release area) that are necessary to meet a particular target. These systems can be fabricated, accordingly, and tested in the laboratory. The analytical forms of $M(\tau)/M(\infty)$ and τ_{eff} make it possible to write optimization routines and determine suitable model parameters. This feature is almost nonexistent in software solely dedicated for simulation of 3-D systems. Another advantage of this analytical framework is the ability to estimate constants, such as the mass transfer coefficient (k_m), from experimental data.

4. Conclusion

Analytical expressions for the cumulative amount of drug released and the effective time constant were derived for a cylindrical matrix system (e.g., implantable devices for pain management). The tube was coated with an impermeable layer so that the active ingredient only escaped through a small rectangular cut. Laplace transforms were applied to develop expressions for the percentage of drug released and the 3-dimensional concentration in the frequency domain. The procedure, completed in Maple, involved several integrations along the radial and axial directions to satisfy the boundary conditions. The Zakian technique was then implemented to obtain the solution. A relaxation time constant was calculated to determine the delivery rate of the medication. As the Sherwood number, or the size of the hole, increased, the drug was removed from the cylinder at a faster rate. Ninety-eight percent (98%) of the loading dose was released after four time constants. The analytical platform may help to estimate physicochemical parameters from laboratory experiments, write design optimization algorithms and fabricate implants for long-term delivery.

Appendix A.

Integration steps

I. Integrating both sides of Eq. (24) with respect to ζ from 0 to H/R and with respect to θ from 0 to 2π leads to

$$\frac{4HI_1(\sqrt{s})\sqrt{s}A_{0,0}\pi}{R} = -\frac{1}{sR}2Shh_0\begin{bmatrix}2iI_1(\sqrt{s})sB_{0,1} + \Theta_0 + 2iI_1(\sqrt{s})sA_{0,1}\sin(\Theta_0)\\ +2I_0(\sqrt{s})A_{0,0}s\Theta_0 - 2iI_1(\sqrt{s})sB_{0,1}\cos(\Theta_0)\end{bmatrix} \tag{A.1}$$

II. Multiplying both sides of Eq. (24) by $\cos(\pi R\zeta/H)$ and integrating with respect to ζ from 0 to H/R and with respect to θ from 0 to 2π, yields

$$\frac{2I_1\left(\frac{\sqrt{\pi^2R^2+sH^2}}{H}\right)\sqrt{\pi^2R^2+sH^2}A_{1,0}\pi}{R} = \frac{1}{sR}2Sh\begin{bmatrix}-iI_1\left(\frac{\sqrt{\pi^2R^2+sH^2}}{H}\right)B_{1,1}\pi h_0 + iI_1\left(\frac{\sqrt{\pi^2R^2+sH^2}}{H}\right)B_{1,1}\sin\left(\frac{\pi h_0}{H}\right)\cos\left(\frac{\pi h_0}{H}\right)H\\ -I_0\left(\frac{\sqrt{\pi^2R^2+sH^2}}{H}\right)A_{1,0}\pi h_0\Theta_0 - iA_{1,1}\pi I_1\left(\frac{\sqrt{\pi^2R^2+sH^2}}{H}\right)h_0\sin(\Theta_0)\\ +iI_1\left(\frac{\sqrt{\pi^2R^2+sH^2}}{H}\right)B_{1,1}\pi h_0\cos(\Theta_0)\\ -iI_1\left(\frac{\sqrt{\pi^2R^2+sH^2}}{H}\right)B_{1,1}\sin\left(\frac{\pi h_0}{H}\right)\cos\left(\frac{\pi h_0}{H}\right)H\cos(\Theta_0)\\ +iI_1\left(\frac{\sqrt{\pi^2R^2+sH^2}}{H}\right)A_{1,1}\sin\left(\frac{\pi h_0}{H}\right)\cos\left(\frac{\pi h_0}{H}\right)H\sin(\Theta_0)\\ +I_0\left(\frac{\sqrt{\pi^2R^2+sH^2}}{H}\right)A_{1,0}\sin\left(\frac{\pi h_0}{H}\right)\cos\left(\frac{\pi h_0}{H}\right)H\Theta_0\end{bmatrix} \tag{A.2}$$

III. Multiplying both sides of Eq. (24) by $\cos(\theta)$ and integrating with respect to ζ from 0 to H/R and with respect to θ from 0 to 2π, gives

$$\frac{2iHA_{0,1}\pi[-I_1(\sqrt{s}) + \sqrt{s}I_0(\sqrt{s})]}{R} = -\frac{1}{sR}2Shh_0[iI_1(\sqrt{s})sB_{0,1} + \sin(\Theta_0) + iI_1(\sqrt{s})sA_{0,1}\cos(\Theta_0)\sin(\Theta_0) + iI_1(\sqrt{s})sA_{0,1}\Theta_0 + 2\sin(\Theta_0)I_0(\sqrt{s})A_{0,0}s - iI_1(\sqrt{s})sB_{0,1}\cos(\Theta_0)^2] \tag{A.3}$$

IV. Multiplying both sides of Eq. (24) by $\sin(\theta)$ and integrating with respect to ζ from 0 to H/R and with respect to θ from 0 to 2π, produces

$$2iHB_{0,1}\pi\frac{[-I_1(\sqrt{s}) + \sqrt{s}I_0(\sqrt{s})]}{R} = \frac{1}{sR}2Shh_0\begin{bmatrix}-1 - iI_1(\sqrt{s})sA_{0,1} - 2I_0(\sqrt{s})A_{0,0}s + \cos(\Theta_0)\\ +iI_1(\sqrt{s})sA_{0,1}\cos(\Theta_0)^2 + 2\cos(\Theta_0)I_0(\sqrt{s})A_{0,0}s\\ +iI_1(\sqrt{s})sB_{0,1}\cos(\Theta_0)\sin(\Theta_0) - iI_1(\sqrt{s})sB_{0,1}\Theta_0\end{bmatrix} \tag{A.4}$$

V. Multiplying both sides of Eq. (24) by $\cos(\theta)\cos(\pi R\zeta/H)$ and integrating with respect to ζ from 0 to H/R and with respect to θ from 0 to 2π, results in

$$-\frac{iA_{1,1\pi}\left[HI_1\left(\frac{\sqrt{\pi^2R^2+sH^2}}{H}\right)-\sqrt{\pi^2R^2+sH^2}I_0\left(\frac{\sqrt{\pi^2R^2+sH^2}}{H}\right)\right]}{R}=$$

$$-\frac{1}{\pi R}Sh\begin{bmatrix} iI_1\left(\frac{\sqrt{\pi^2R^2+sH^2}}{H}\right)B_{1,1}\pi h_0-iI_1\left(\frac{\sqrt{\pi^2R^2+sH^2}}{H}\right)B_{1,1}\sin\left(\frac{\pi h_0}{H}\right)\cos\left(\frac{\pi h_0}{H}\right)H \\ +2I_0\left(\frac{\sqrt{\pi^2R^2+sH^2}}{H}\right)A_{1,0}\pi h_0\sin(\Theta_0)+iI_1\left(\frac{\sqrt{\pi^2R^2+sH^2}}{H}\right)A_{1,1}\pi h_0\cos(\Theta_0)\sin(\Theta_0) \\ +iI_1\left(\frac{\sqrt{\pi^2R^2+sH^2}}{H}\right)A_{1,1}\pi h_0\Theta_0-iI_1\left(\frac{\sqrt{\pi^2R^2+sH^2}}{H}\right)B_{1,1}\pi h_0\cos(\Theta_0)^2 \\ +iI_1\left(\frac{\sqrt{\pi^2R^2+sH^2}}{H}\right)B_{1,1}\sin\left(\frac{\pi h_0}{H}\right)\cos\left(\frac{\pi h_0}{H}\right)H\cos(\Theta_0)^2 \\ -iI_1\left(\frac{\sqrt{\pi^2R^2+sH^2}}{H}\right)A_{1,1}\sin\left(\frac{\pi h_0}{H}\right)\cos\left(\frac{\pi h_0}{H}\right)H\cos(\Theta_0)\sin(\Theta_0) \\ -iI_1\left(\frac{\sqrt{\pi^2R^2+sH^2}}{H}\right)A_{1,1}\sin\left(\frac{\pi h_0}{H}\right)\cos\left(\frac{\pi h_0}{H}\right)H\Theta_0 \\ -2I_0\left(\frac{\sqrt{\pi^2R^2+sH^2}}{H}\right)A_{1,0}\sin\left(\frac{\pi h_0}{H}\right)\cos\left(\frac{\pi h_0}{H}\right)H\sin(\Theta_0) \end{bmatrix} \tag{A.5}$$

VI. Multiplying both sides of Eq. (24) by $\sin(\theta)\cos(\pi R\zeta/H)$ and integrating with respect to ζ from 0 to H/R and with respect to θ from 0 to 2π, leads to

$$-\frac{iB_{1,1\pi}\left[HI_1\left(\frac{\sqrt{\pi^2R^2+sH^2}}{H}\right)-\sqrt{\pi^2R^2+sH^2}I_0\left(\frac{\sqrt{\pi^2R^2+sH^2}}{H}\right)\right]}{R}=$$

$$-\frac{1}{\pi R}Sh\begin{bmatrix} 2I_0\left(\frac{\sqrt{\pi^2R^2+sH^2}}{H}\right)A_{1,0}\pi h_0+iI_1\left(\frac{\sqrt{\pi^2R^2+sH^2}}{H}\right)A_{1,1}\pi h_0 \\ -iI_1\left(\frac{\sqrt{\pi^2R^2+sH^2}}{H}\right)A_{1,1}\sin\left(\frac{\pi h_0}{H}\right)\cos\left(\frac{\pi h_0}{H}\right)H \\ -2I_0\left(\frac{\sqrt{\pi^2R^2+sH^2}}{H}\right)A_{1,0}\sin\left(\frac{\pi h_0}{H}\right)\cos\left(\frac{\pi h_0}{H}\right)H \\ -2\cos(\Theta_0)I_0\left(\frac{\sqrt{\pi^2R^2+sH^2}}{H}\right)A_{1,0}\pi h_0-iI_1\left(\frac{\sqrt{\pi^2R^2+sH^2}}{H}\right)A_{1,1}\pi h_0\cos(\Theta_0)^2 \\ -iI_1\left(\frac{\sqrt{\pi^2R^2+sH^2}}{H}\right)B_{1,1}\pi h_0\cos(\Theta_0)\sin(\Theta_0)+iI_1\left(\frac{\sqrt{\pi^2R^2+sH^2}}{H}\right)B_{1,1}\pi h_0\Theta_0 \\ +iI_1\left(\frac{\sqrt{\pi^2R^2+sH^2}}{H}\right)B_{1,1}\sin\left(\frac{\pi h_0}{H}\right)\cos\left(\frac{\pi h_0}{H}\right)H\cos(\Theta_0)\sin(\Theta_0) \\ -iI_1\left(\frac{\sqrt{\pi^2R^2+sH^2}}{H}\right)B_{1,1}\sin\left(\frac{\pi h_0}{H}\right)\cos\left(\frac{\pi h_0}{H}\right)H\Theta_0 \\ +iI_1\left(\frac{\sqrt{\pi^2R^2+sH^2}}{H}\right)A_{1,1}\sin\left(\frac{\pi h_0}{H}\right)\cos\left(\frac{\pi h_0}{H}\right)H\cos(\Theta_0)^2 \\ +2\cos(\Theta_0)I_0\left(\frac{\sqrt{\pi^2R^2+sH^2}}{H}\right)A_{1,0}\sin\left(\frac{\pi h_0}{H}\right)\cos\left(\frac{\pi h_0}{H}\right)H \end{bmatrix} \tag{A.6}$$

References

Ainaoui, A., Siepmann, J., Bodmeier, R., Vergnaud, J.M., 2001. Calculation of the dimensions of dosage forms with release controlled by diffusion for in vivo use. Eur. J. Pharm. Biopharm. 51, 17–24.

Bunge, A.L., 1998. Release rates from topical formulations containing drugs in suspension. J. Control. Release 52, 141–148.

Collins, R., 1980. The choice of an effective time constant for diffusive processes in finite systems (thermal conduction and sputtering examples). J. Phys. D: Appl. Phys. 13, 1935.

Crank, J., 1975. The Mathematics of Diffusion, second ed. Clarendon Press, Oxford, England.

Davia, L., Grassi, G., Pontrelli, G., Lapasin, R., Perin, D., Grassi, M., 2009. Mathematical modelling of NABD release from endoluminal gel paved stent. Comput. Biol. Chem. 33, 33–40.

Ertan, G., Karasulu, E., Demirtas, D., Arici, M., Guneri, T., 1997. Release characteristics of implantable cylindrical polyethylene matrices. J. Pharm. Pharmacol. 49, 229–235.

Fernandes, M., Simon, L., Loney, N.W., 2005. Mathematical modeling of transdermal drug-delivery systems: analysis and applications. J. Membr. Sci. 256, 184–192.

Frenning, G., Brohede, U., Stromme, M., 2005. Finite element analysis of the release of slowly dissolving drugs from cylindrical matrix systems. J. Control. Release 107, 320–329.

Guy, R.H., Hadgraft, J., 1980. A theoretical description relating skin penetration to the thickness of the applied medicament. Int. J. Pharm. 6, 321–332.

Higuchi, T., 1961. Rate of release of medicaments from ointment bases containing drugs in suspension. J. Pharm. Sci. 50, 874–875.

Hsu, J.P., Ting, C., Lin, M.J., 1992. A theoretical analysis of a new drug delivery system: a cylindrical device with a vertical opening on its surface. J. Pharm. Sci. 81, 866–870.

Kalia, Y.N., Guy, R.H., 2001. Modeling transdermal drug release. Adv. Drug Deliv. Rev. 48, 159–172.

Kim, C.J., 2000. Controlled Release Dosage Form Design, first ed. Technomic Publishing Co., Lancaster, PA.

Korsmeyer, R.W., Lustig, S.R., Peppas, N.A., 1986. Solute and penetrant diffusion in swellable polymers. I. Mathematical modeling. J. Polym. Sci. B: Polym. Phys. 24, 395–408.

Lin, C.C., Metters, A.T., 2006. Hydrogels in controlled release formulations: network design and mathematical modeling. Adv. Drug Deliv. Rev. 58, 1379–1408.

Loney, N.W., 2007. Applied Mathematical Methods for Chemical Engineers, second ed. CRC/Taylor & Francis, Boca Raton, FL.

Patel, M.M., Shah, T.J., Amin, A.F., Shah, N.N., 2009. Design, development and optimization of a novel time and pH-dependent colon targeted drug delivery system. Pharm. Dev. Technol. 14, 62–69.

Prasanna, R.I., Sankari, K.U., 2012. Design, evaluation and in vitro–in vivo correlation of glibenclamide buccoadhesive films. Int. J. Pharm. Invest. 2, 26–33.

Rastogi, A., Bowman, P., Stavchansky, S., 2012. Evaluation of a perforated drug delivery system in mice for prolonged and constant release of a hydrophilic drug. Drug Deliv. Transl. Res. 2, 106–111.

Rastogi, A., Luo, Z., Wu, Z., Ho, P.S., Bowman, P.D., Stavchansky, S., 2010. Development and characterization of a scalable microperforated device capable of long-term zero order drug release. Biomed. Microdevices 12, 915–921.

Rice, R.G., Do, D.D., 1995. Applied Mathematics and Modeling for Chemical Engineers. Wiley, New York.

Ritger, P.L., Peppas, N.A., 1987. A simple equation for description of solute release II. Fickian and anomalous release from swellable devices. J. Control. Release 5, 37–42.

Siepmann, J., Podual, K., Sriwongjanya, M., Peppas, N.A., Bodmeier, R., 1999. A new model describing the swelling and drug release kinetics from hydroxypropyl methylcellulose tablets. J. Pharm. Sci. 88, 65–72.

Simon, L., 2009. Timely drug delivery from controlled-release devices: dynamic analysis and novel design concepts. Math. Biosci. 217, 151–158.

Simon, L., Ospina, J., 2012. Two-dimensional solution and analysis of a cylindrical matrix device with a circular release area. Chem. Eng. Commun. 200, 115–138.

Tojo, K., Miyanami, K., 1983. Controlled release from a cylindrical matrix device. Bull. Univ. Osaka Pref. Ser. A 31, 149–157.

Vergnaud, J.M., Rosca, I.-D., 2005. Assessing Bioavailability of Drug Delivery Systems: Mathematical and Numerical Treatment. CRC: Taylor & Francis, Boca Raton, FL.

Verma, P.R., Iyer, S.S., 2000. Controlled transdermal delivery of propranolol using HPMC matrices: design and in-vitro and in-vivo evaluation. J. Pharm. Pharmacol. 52, 151–156.

Zhao, H.Q., Jayasinghe, D., Hossainy, S., Schwartz, L.B., 2012. A theoretical model to characterize the drug release behavior of drug-eluting stents with durable polymer matrix coating. J. Biomed. Mater. Res. A 100, 120–124.